Structural Asymmetries in the Human Brain: a Voxel-based Statistical Analysis of 142 MRI Scans

K.E. Watkins[1], T. Paus[1], J.P. Lerch[1,2], A. Zijdenbos[2], D.L. Collins[2], P. Neelin[2], J. Taylor[3], K.J. Worsley[3] and A.C. Evans[2]

[1]Cognitive Neuroscience Unit, Montreal Neurological Institute, McGill University, [2]McConnell Brain Imaging Centre, Montreal Neurological Institute, McGill University and [3]Department of Maths and Statistics, McGill University, Montreal, Quebec, Canada

The use of computational approaches in the analysis of high-resolution magnetic resonance images (MRI) of the human brain provides a powerful tool for *in vivo* studies of brain anatomy. Here, we report results obtained with a voxel-wise statistical analysis of hemispheric asymmetries in regional 'amounts' of gray matter, based on MRI scans obtained in 142 healthy young adults. Firstly, the voxel-wise analysis detected the well-known frontal (right > left) and occipital (left > right) petalias. Secondly, our analysis confirmed the presence of left-greater-than-right asymmetries in several posterior language areas, including the planum temporale and the angular gyrus; no significant asymmetry was detected in the anterior language regions. We also found previously described asymmetries in the cingulate sulcus (right > left) and the caudate nucleus (right > left). Finally, in some brain regions we observed highly significant asymmetries that were not reported before, such as in the anterior insular cortex (right > left). The above asymmetries were observed in men and women. Our results thus provide confirmation of the known structural asymmetries in the human brain as well as new findings that may stimulate further research of hemispheric specialization.

Introduction

The hemispheres of the human brain are functionally and structurally asymmetric. The best-known functional asymmetry is that of left-hemisphere specialization for language (Broca, 1861). The discovery of a structural asymmetry between the left and right plana temporale (Geschwind and Levitsky, 1968), favoring the left hemisphere and coinciding spatially with a region of the brain known to subserve language, suggested that the study of structural asymmetries might provide important clues to the neuroanatomical basis of lateralized brain functions.

The analysis of structural asymmetries is also of use in identifying the neuroanatomical basis of disorders with a presumed developmental etiology, such as dyslexia, autism and schizophrenia (Crow, 1990; Filipek, 1995; Petty, 1999; Sharma *et al.*, 1999; Hendren *et al.*, 2000). The underlying assumption in such studies is that abnormal brain development results in atypical structural asymmetries, which in turn are related to abnormal functional organization.

The asymmetry of the planum temporale was revealed initially by analysis of post-mortem specimens. Analysis of skulls and computed tomography brain scans revealed other asymmetries, namely the extension of the frontal lobe in the right hemisphere and the occipital lobe in the left hemisphere (LeMay, 1977; Chui and Damasio, 1980; LeMay, 1984). These asymmetries have become known as the frontal and occipital 'petalias', a term originally used to refer to the indentation made on the inner table of the skull by these extensions. These extensions could be related to a spatial displacement of the left and right hemispheres with respect to each other rather than to a difference in the amount of tissue in these regions. Similarly for the planum temporale, it has been suggested that the apparent difference in size between the left and right hemispheres is related to a shape asymmetry of the posterior Sylvian fissure (Westbury *et al.*, 1999). Several morphometric studies using magnetic resonance imaging (MRI), have also described the presence of right frontal and left occipital petalias and the leftward asymmetry of the planum temporale (Falk *et al.*, 1991; Steinmetz and Galaburda, 1991). Similarly, several volumetric region-of-interest MRI studies of clinical populations have revealed abnormal asymmetries of many brain structures [for reviews see (Filipek, 1995; Hendren *et al.*, 2000)].

These morphometric studies are labor-intensive and typically focus on one or two regions-of-interest. Also, they suffer from difficulties related to defining structural anatomical boundaries; gross morphological landmarks such as cerebral sulci are variable in their presence and location. Such difficulties can result in low intra- and inter-rater reliability. There is a need, therefore, for a whole-brain imaging analysis that is both reproducible and automated. One such method, a voxel-based statistical analysis of the amounts of gray and white matter (Wright *et al.*, 1995; Vargha-Khadem *et al.*, 1998; Paus *et al.*, 1999; Ashburner and Friston, 2000), is well suited for examining structural hemispheric asymmetries. This analysis of MRI brain volumes uses computer-based spatial transformations to remove differences due to brain size and automated algorithms to classify tissues. The latter removes the need for subjective identification of tissue boundaries, a potential source of error in many manual analyses.

We used voxel-based analyses to examine structural asymmetries throughout the whole brain in a population of 142 healthy adults. MRI brain volumes were acquired in each subject and processed to create maps of the difference in the amounts of gray matter between the two hemispheres. The difference images were statistically analyzed on a voxel-by-voxel basis. Although previous studies have used automated analyses of deformation fields to examine shape differences between the left and right hemispheres (Ashburner *et al.*, 1998; Prima *et al.*, 1998), to our knowledge, this is the first fully automated analysis of cerebral asymmetries in regional amounts of gray matter, which also has the advantage of being unbiased with respect to focusing on specific regions-of-interest. Such an analysis provides the opportunity to discover asymmetries that have not been reported previously because of difficulties in the definition of anatomical boundaries.

Materials and Methods

The subjects scanned were 152 unselected normal volunteers. Each subject gave written informed consent; the Research Ethics Committee of the Montreal Neurological Institute and Hospital approved the study. The scans of 10 subjects were excluded because their handedness was not known. Of the remaining 142 subjects, 81 were male and 61 were female. Ages ranged from 18 to 44 years (mean age 24.82, SD 4.81). On a short handedness questionnaire, 14 subjects were dominant for left-hand use

on a number of tasks; the remaining 128 subjects preferred to use their right hand.

Each subject was scanned using MRI on a Phillips Gyroscan 1.5 T superconducting magnet system. Three sequences were used, yielding T_1-weighted (3D fast field echo scan with 140–160 slices, 1 mm isotropic resolution, T_R = 18 ms, T_E = 10 ms, flip angle = 30°), T_2-weighted (2D multi-slice fast spin echo scan with 140–160 2 mm slices with a 1 mm overlap, T_R = 3300 ms, T_E = 35 ms) and proton density (as for T_2 scan, but with T_E = 120 ms) image volumes of the whole head. Each image volume underwent a non-uniformity correction (Sled *et al.*, 1998) to remove variations in signal intensity related to radio-frequency inhomogeneity. The 142 T_1-weighted brain volumes were stereotaxically transformed using nine parameters (Collins *et al.*, 1994) to match the Montreal Neurological Institute 305 average template (MNI305). These 142 T_1-weighted linearly transformed image volumes and their mirror images were averaged to create a new symmetrical template. This new template was created because the MNI305 template is structurally asymmetric and may introduce or increase asymmetry of the original data. The MNI305 template is an average of 305 brain scans and thus reflects the average asymmetry of such a population; for example, the frontal and occipital petalias are clearly seen in this template. Each original T_1-weighted, T_2-weighted and proton density image volume was then linearly transformed to match the new symmetrical template. This transformation effectively normalized the volumes for between-subject differences in brain size and aligns the images in the standardized stereotaxic space of Talairach and Tournoux (1988). Transformation to a symmetrical template also improved the spatial homology between the two hemispheres in each subject. The symmetrically transformed images were then classified into gray matter, white matter and cerebrospinal fluid by means of INSECT (Zijdenbos *et al.*, 1998), an automatic tissue-classification algorithm. Briefly, INSECT relies on an artificial neural network classifier, which labels each voxel based on the MRI signal in each of the three (T_1-, T_2-, and proton density weighted) input MRI volumes. The classifier was trained for each brain volume by providing it with the coordinates of voxels that have a minimum likelihood of 90% for belonging to one of the target tissue classes. A binary mask of gray matter voxels was extracted from the classified image and smoothed using a Gaussian smoothing kernel of 10 mm full-width at half-maximum. Smoothing serves a number of purposes: it converts the binary data into a range of continuous data, which is required for the statistical analyses used in this study; it weights the signal at each voxel according to the signal in neighboring voxels, thereby reflecting the amount of gray matter within the smoothing kernel (i.e. its regional density or concentration); and it reduces the effect of spatial differences between hemispheres and also that of between-subject differences in the exact spatial location of gyri and sulci. Thus, the analysis of smoothed data, combined with the large number of brains analyzed and the use of a symmetric template, reduces the likelihood of finding a false positive asymmetry. Smoothing the data also increases the detection of asymmetries whose spatial extent matches the width of the smoothing kernel (i.e. 10 mm in our study) and increases the validity of the Gaussian assumption, making the false positive rates more accurately determined. The probability of false negative findings is high, however, because the use of a symmetric template might increase the symmetry of the brains, also because differences with spatial extents smaller than the size of the smoothing kernel may not be detected, but mainly because of the stringent statistical correction for multiple comparisons. Negative findings should, therefore, be interpreted cautiously.

In order to examine within-subject cerebral asymmetries, a new set of images was generated by flipping each smoothed gray matter volume about the parasagittal plane through x = 0 (i.e. the midline), thereby creating a mirror image. In each subject, this mirror image was subtracted voxel-by-voxel from the unflipped smoothed gray matter image to create an image representing the differences in the amount of gray matter between the two hemispheres. The longitudinal fissure might not coincide exactly with the parasagittal plane through x = 0, however, particularly in its posterior portion; differences in the midline, therefore, must be considered with caution. Even so, the most common deviation of the posterior midline is toward the right (i.e. a larger left occipital region), which would result in more gray matter erroneously being assigned to the right hemisphere and an unexpected finding of a rightward asymmetry or an underestimate of the expected leftward asymmetry.

In the difference images, positive voxel values on the left side of the image indicated that the left hemisphere had higher signal (i.e. more gray matter) than the right, and positive voxel values on the right side of the image indicated that the right hemisphere had higher signal than the left. These images were then analyzed using a *t*-test at each voxel. A threshold for the *t*-statistic of >5.0 was calculated (Worsley *et al.*, 1996) based on 141 degrees of freedom, a voxel size of 1 mm^3, smoothness of 10 mm, a volume of interest of 1000 cc, and a significance level of $P < 0.05$, corrected for multiple comparisons. It should be noted that the cerebellum was masked (i.e. its signal was removed) in the MRI volumes during these analyses and, therefore, only differences in cerebral gray matter were analyzed.

Results

The individual subject maps indicating the difference in the amount of gray matter between the left and right hemispheres were averaged and the mean differences were superimposed onto a single brain image (see Fig. 1*a*). Examination of this map reveals that, on average, there is more gray matter in the right frontal lobe compared to the left, and conversely in the left occipital lobe compared to the right. Although the average within-subject difference between the two hemispheres can be large, if between-subject variance in this difference is also large (see Fig. 1*b*), the difference might not achieve statistical significance in the group analysis. To calculate the statistical significance of these differences, a *t*-statistic was derived at each voxel by dividing the mean difference by the standard error of the mean (i.e. a one-sample *t*-test; Fig. 1*c*).

This statistical analysis of gray matter differences between the left and right hemispheres confirmed the general pattern observed in the map of mean differences (Fig. 1*a*) and the presence of the most robust asymmetries in the brain, namely the right frontal and left occipital petalias (see Fig. 2). Left-greater-than-right ($L > R$) asymmetries are shown in Table 1 and right-greater-than-left ($R > L$) asymmetries are shown in Table 2. Examination of Table 2 reveals that a large number of significant statistical 'peaks' were located in anterior regions of the right hemisphere (indicating $R > L$ asymmetry in the amount of gray matter), with none in the right occipital lobe. Examination of Table 1 reveals that several significant peaks were located in posterior regions of the left hemisphere, including the left occipital and parietal lobes (indicating $L > R$ asymmetry in the amount of gray matter). The most statistically significant difference was located in the right frontal pole and a number of other significant peaks were located in the right superior and middle frontal gyri, particularly in mid-dorsolateral frontal cortex, confirming previous findings that this lobe extends further anteriorly and laterally in the right hemisphere than in the left (see Fig. 2*a* and *b*). The most statistically significant difference favoring the left hemisphere was located in the occipital pole; this asymmetry extended to the lateral surface of the superior parietal lobe to include the angular gyrus and intraparietal sulcus (see Fig. 2*b* and *c*). The $L > R$ asymmetry of the planum temporale was also found to be significant (see Fig. 3).

For each subject, the value of the voxels at the statistical peaks located in the frontal and occipital petalias (respectively, right superior frontal gyrus: coordinates 11, 59, 24; and, left superior occipital gyrus: coordinates –14, –86, 32), and planum temporale (coordinates: –35, –38, 12) were extracted from the difference image and graphed to examine their distributions and compare them with those previously reported (see Fig. 4). The distributions for the three asymmetries were qualitatively similar to those calculated previously in post-mortem specimens (Geschwind and Levitsky, 1968) and computed tomography

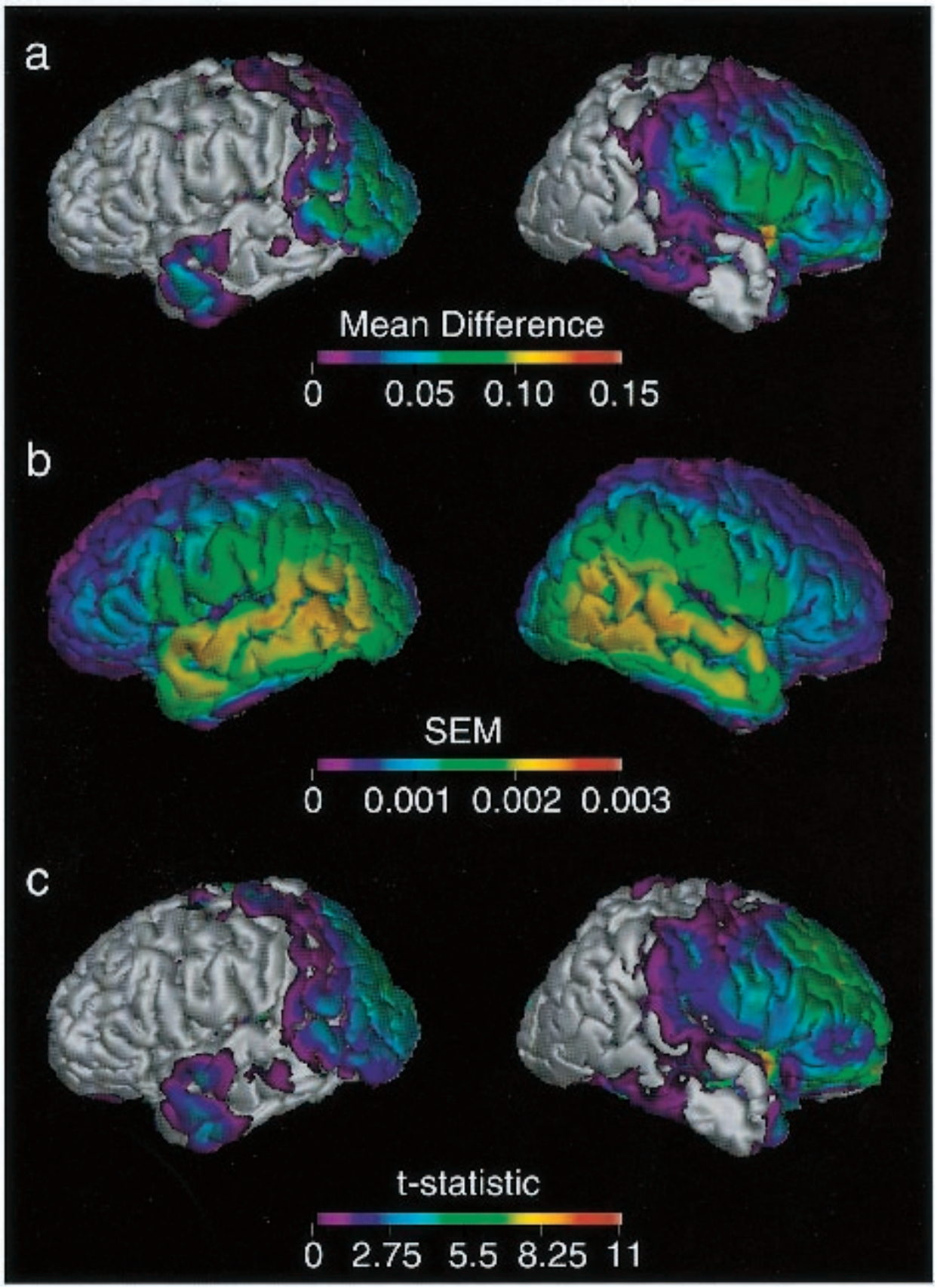
a
Mean Difference
0 0.05 0.10 0.15
b
SEM
0 0.001 0.002 0.003
c
t-statistic
0 2.75 5.5 8.25 11

Table 1
Leftward gray matter asymmetries (i.e. L > R)

Anatomical region	BA	*X*	*Y*	*Z*	*t*-statistic[a]			
					All subjects	Right-handed subjects	Male subjects	Female subjects
Frontal lobe								
Anterior orbital gyrus	13	–26	45	–7	**5.74**	9.15	6.05	7.93
Lateral orbital sulcus	11	–39	38	–8	**7.75**	8.48	5.84	8.93
Superior rostral sulcus	32	–5	29	–15	**5.29**	6.54		5.44
Anterior insula (superior)	–	–30	18	11	**5.29**	9.27	5.80	8.35
Middle insula (very medial)[b]	–	–29	11	–6	**5.44**	9.35	7.31	7.51
Inferior precentral sulcus	6	–51	–3	17	**5.45**		6.09	
	6	–40	–4	23	**5.24**	7.18	6.00	5.54
Superior precentral gyrus	6	–1	–7	72	**5.60**			
	6	–24	–10	62	**6.02**	9.78		
	6	–12	–23	71	**6.56**	9.62	8.28	7.04
	6	–11	–36	66	**5.93**	9.17	8.57	6.76
Subcortical structures								
Lateral, posterior thalamus/putamen	–	–26	–24	1	**6.74**	8.91	10.14	5.58
	–	–26	–31	15	**5.71**	8.53		8.16
Temporal lobe								
Planum temporale	42/22	–35	–38	12	**7.25**	9.17	9.26	7.47
Posterior fusiform gyrus	37	–36	–51	–11	**5.82**	10.07	5.74	9.21
Parietal lobe								
Intraparietal sulcus	7a/b	–21	–69	54	**7.68**	6.85	8.91	5.37
Angular gyrus	39	–36	–83	43	**5.06**	8.28		
Occipital lobe								
Calcarine sulcus	17	–15	–66	0	**8.53**	11.60	9.48	8.35
	17	–31	–70	1	**6.36**			8.37
Superior occipital gyrus	19	–14	–86	32	**8.78**	10.36	9.73	7.09
	19	–12	–99	18	**6.55**	9.52	7.54	7.25

BA – Brodmann's area; *X, Y, Z* – Talairach coordinates. The *t*-statistics for the results of the analysis of 142 subjects are highlighted in bold; *t*-statistics for the same peaks in three subsequent analyses of right-handed subjects only ($n = 128$), male subjects only ($n = 81$) and female subjects only ($n = 61$) are shown alongside for comparison.

[a]*t*-statistic > 5.00 ($P < 0.05$ corrected for multiple comparisons).

[b]Peak lies close to claustrum and putamen.

scans (LeMay, 1984), but chi-squared analyses revealed significant differences between the sets of distributions for the planum temporale ($\chi^2 = 26.18$, $P < 0.001$) and the frontal petalia ($\chi^2 = 44.45$, $P < 0.001$). These differences were mainly due to discrepancies in the number of subjects assessed to have symmetry ($L = R$) in the different analyses; previous analyses may have estimated a larger number of such subjects possibly because of differences in the resolution of the measurements made in comparison with those made in our analyses.

Several other asymmetries were revealed by our analysis (see Tables 1 and 2). The amounts of gray matter in the posterior fusiform gyrus (Fig. 3*a*), the lateral orbital sulcus (Fig. 3*a*), the superior–rostral sulcus of the medial frontal lobe, inferior and superior portions of the precentral gyrus (Fig. 2*b*), and a superior portion of the anterior insula demonstrated $L > R$ asymmetries. Conversely, the amount of gray matter in the anterior cingulate sulcus (Fig. 5), inferior portion of the anterior insula (Fig. 6*a*), frontal operculum (Fig. 6*b*,*c*), uncus (Fig. 2*c*), superior temporal sulcus (Fig. 6*b*,*c*), inferior temporal gyrus (Fig. 6*b*,*c*) and parietal–occipital fissure (Fig. 5*a*–*c*) demonstrated $R > L$ asymmetries. Subcortically, the putamen and lateral thalamus demonstrated $L > R$ asymmetry (see Table 1), whereas the caudate nucleus (Fig. 5*a*–*c*) and dorsal thalamus demonstrated $R > L$ asymmetry (see Table 2).

Further voxel-wise analyses compared the degree of asymmetry between male and female subjects (81 and 61 subjects, respectively) and between left- and right-handed subjects (14 and 128 subjects, respectively). The interaction between sex and handedness was also examined. None of these analyses produced statistically significant results, following corrections for multiple comparisons. As noted earlier, the statistical correction for multiple comparisons is likely to result in a high number of false negatives. The data were reanalyzed for the right-handed subjects ($n = 128$) only and for the male ($n = 81$) and female subjects ($n = 61$) separately. These analyses produced similar patterns of results to the whole group analysis of all 142 subjects (see Tables 1 and 2). Nevertheless, for the analysis of right-handed subjects only, there were large increases in the *t*-statistics for the same peaks found to be significant in the analysis of all 142 subjects. Similarly, for the analysis of male subjects only, increases in the *t*-statistics were observed most noticeably in the right frontal lobes. This was not the case for the analysis of female subjects only.

Discussion

Our analysis of the MRI brain volumes in a large sample of healthy young adults revealed the well-known right frontal and left occipital petalias, and $L > R$ asymmetry of the planum temporale. We have also replicated previously described asymmetries, such as $R > L$ cingulate sulcus and caudate nucleus, and

Figure 1. Structural cerebral asymmetries of gray matter volume. Maps reflecting (*a*) mean inter-hemispheric differences in the amounts of gray matter, (*b*) standard error of the mean (SEM) and (*c*) *t*-statistics are superimposed on a surface-rendered image of a single subject. A 24-year-old, right-handed, male subject was selected from the population to represent the median age and handedness score of the subjects. The left hemisphere is shown on the left and the right hemisphere on the right. The maps were thresholded at zero to indicate positive differences and *t*-values (a positive difference or *t*-value in the right hemisphere indicates $R > L$ whereas in the left hemisphere it indicates $L > R$). Note that the map of the SEM is calculated from the sum of squares and therefore its values are positive in both hemispheres.

Table 2
Rightward gray matter asymmetries (i.e. R > L)

Anatomical region	BA	*X*	*Y*	*Z*	*t*-statistic[a]			
					All subjects	Right-handed subjects	Male subjects	Female subjects
Frontal lobe								
Superior frontal gyrus	10	14	64	14	**7.79**		13.04	7.96
	10	11	59	24	**10.74**	15.05	13.16	11.10
	9	21	56	28	**7.11**		12.85	5.62
	9	8	47	37	**8.01**	13.64	13.81	
	8/9	32	35	45	**7.21**			7.00
	8	25	27	60	**5.49**			
	6/8	7	27	49	**6.68**	13.01	9.57	9.28
	6/8	30	20	53	**5.29**	7.68	8.22	
	6	12	–3	53	**5.34**		5.67	6.17
Anterior orbital gyrus	10	22	63	–13	**7.76**	11.89	9.86	8.83
Medial orbital gyrus	10/11	18	47	–18	**5.78**	8.43	5.81	7.75
Middle frontal gyrus	10	33	58	–1	**8.14**	10.51	11.52	6.66
	10	26	58	20	**6.50**	10.55		
	9/46d	33	54	16	**7.65**	11.35	10.37	
	9/46d	34	51	23	**7.25**	11.28	11.31	6.60
	9/46d	30	45	36	**7.50**	11.96	11.72	5.86
	9/46d	37	45	27	**7.15**			7.52
	9/46d	50	35	13	**5.74**			
	9/46d	53	31	22	**5.12**	7.72	6.55	5.09
Cingulate sulcus (anterior)	24	9	41	10	**5.29**	9.35	7.53	7.87
	24	11	21	39	**5.93**	10.11		
	24	9	16	41	**5.98**			7.26
Anterior insula (very inferior)[b]	–	42	8	–13	**10.20**	13.04	12.22	9.41
Frontal operculum (premotor)	6	51	4	–4	**9.00**	10.65		7.88
Subcortical regions								
Head of caudate nucleus	–	14	21	6	**8.14**	11.98	9.51	9.75
Dorsal thalamus	–	3	–5	13	**6.69**	8.37	6.59	7.64
Temporal lobe								
Uncus	28	24	8	–39	**5.52**	7.83		6.19
Superior temporal sulcus	22	49	–16	–13	**7.58**	11.35	8.64	9.38
	22	50	–29	–3	**6.43**	10.46	7.75	8.77
Inferior temporal gyrus	37/19	47	–50	–26	**6.26**	11.8	8.06	9.22
Parietal lobe								
Parietal-occipital fissure	23/30	16	–56	12	**5.52**	7.93	6.35	6.62

See legend to Table 1 for further details.

[a]*t*-statistic > 5.00 ($P < 0.05$ corrected for multiple comparisons).

[b]Falciform fold.

identified new asymmetries, such as $R > L$ anterior insula. In the initial analysis, no significant differences in the degree of asymmetry were observed between male and female subjects or between left- and right-handed subjects. Subsequent re-analyses of the right-handed subjects only and the male subjects only, revealed increases in the *t*-statistics for some of the asymmetries revealed by the initial whole-group analysis, suggesting a trend toward increased asymmetries in these separate groups. We will address some specific issues pertaining to the method used to examine asymmetry before discussing these results.

The methods of voxel-based analyses of structural imaging data have been described in detail by Ashburner and Friston (Ashburner and Friston, 2000). Our analysis differs slightly in that we used a multispectral image-acquisition protocol to obtain T_1-, T_2- and proton-density weighted images in each subject. The advantage of the multispectral approach is that it increases the accuracy of tissue classification by providing the classifier with information regarding signal intensity from sequences sensitive to different classes of tissue. Previous studies, however, have successfully analyzed images obtained using only T_1-weighted acquisition protocols (Vargha-Khadem *et al.*, 1998; Paus *et al.*, 1999).

The analysis of asymmetry required an additional processing step: mirror images were created and subtracted from the original smoothed gray-matter images, resulting in images reflecting within-subject (between hemisphere) differences in

Figure 2. Gray matter asymmetry in the frontal and occipital petalias. The map of the *t*-statistic was thresholded at >3.0 and superimposed on a surface-rendered image of a single subject (see Fig. 1 for details). (*a*) View of the right frontal lobe indicating $R > L$ asymmetry extending from the orbital surface onto the lateral convexity. Note also the highly significant peak in the insula region, buried in the Sylvian fissure, and the peaks buried in the superior temporal sulcus. (*b*) View of the dorsal surface of both hemispheres indicating the $R > L$ frontal and $L > R$ occipital asymmetries. Note also the $L > R$ asymmetry of the precentral region. (*c*) View of the left occipital lobe indicating $L > R$ asymmetry extending from the pole onto the lateral surface to include the angular and intraparietal gyri. The $R > L$ asymmetries of the inferior temporal gyrus and uncus are also visible on the ventral surface of the right temporal lobe.

Figure 3. Asymmetry of the planum temporale. The map of the *t*-statistic was thresholded at >4.0 and superimposed on sagittal slices through the MRI brain volume of a single subject. The slices shown are from the lateral left hemisphere; values of *x* are given in the upper right corner of each image, indicating the distance (in mm) of the image from the parasagittal plane through the midline. Note the position of the statistical peak indicating $L > R$ asymmetry of the planum temporale: it lies just posterior to the transverse gyrus and extends laterally. Note also the $L > R$ asymmetry in the lateral orbital sulcus and posterior fusiform gyrus (*a*, *b* and *c*).

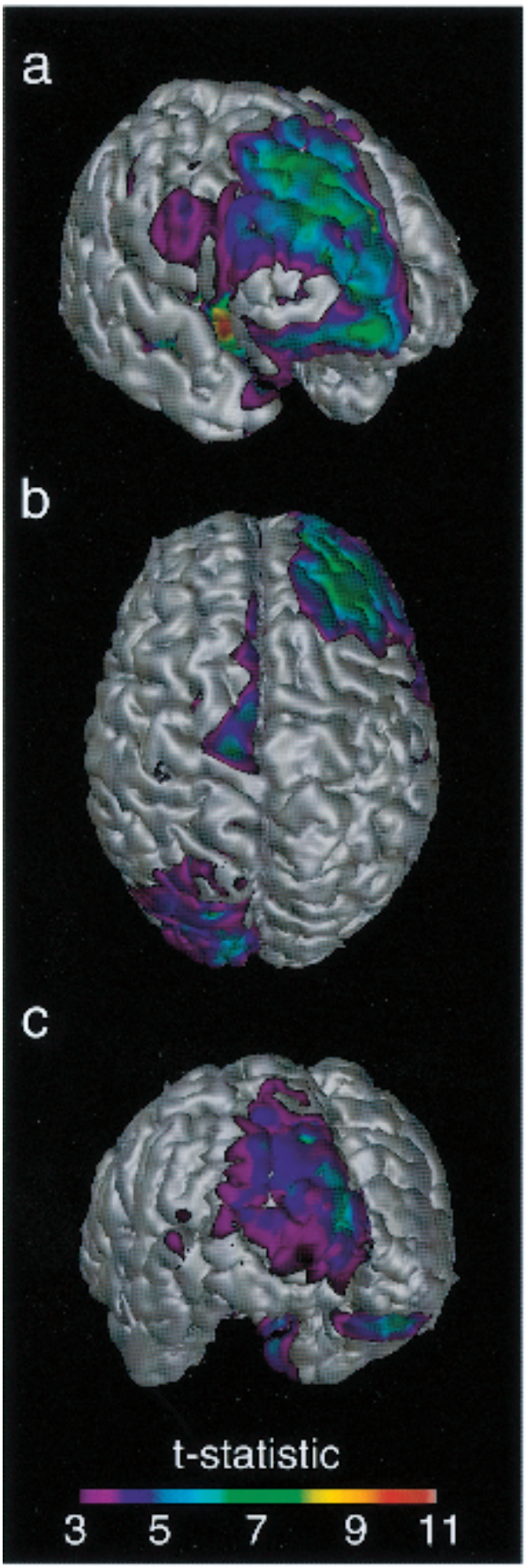

Figure 2

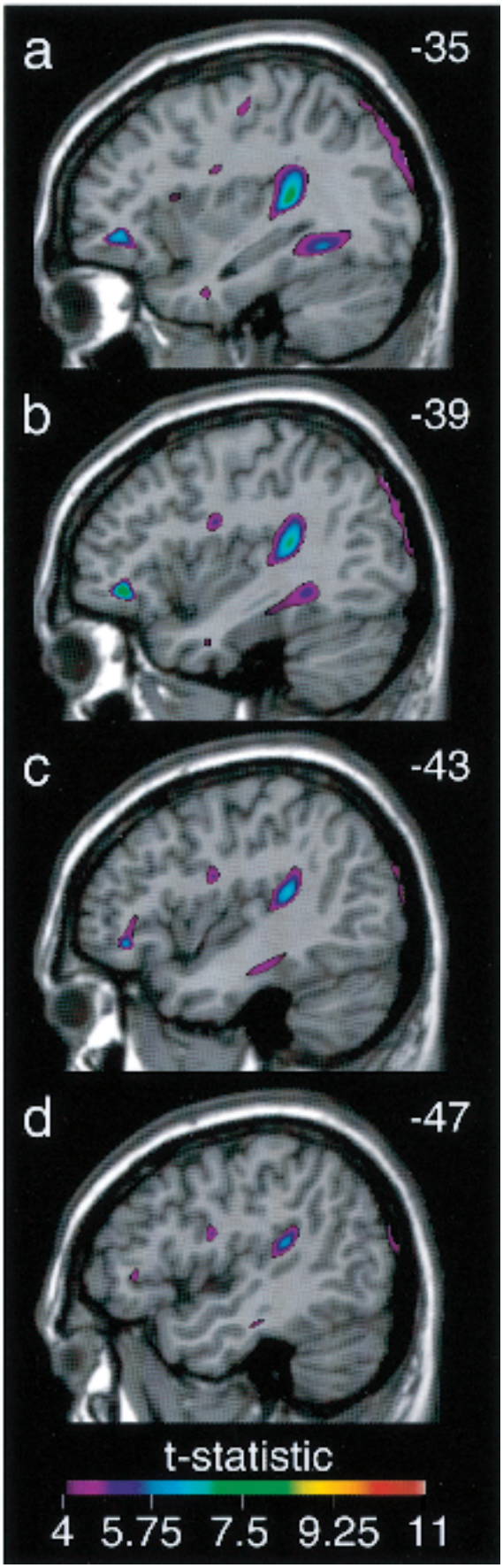

Figure 3

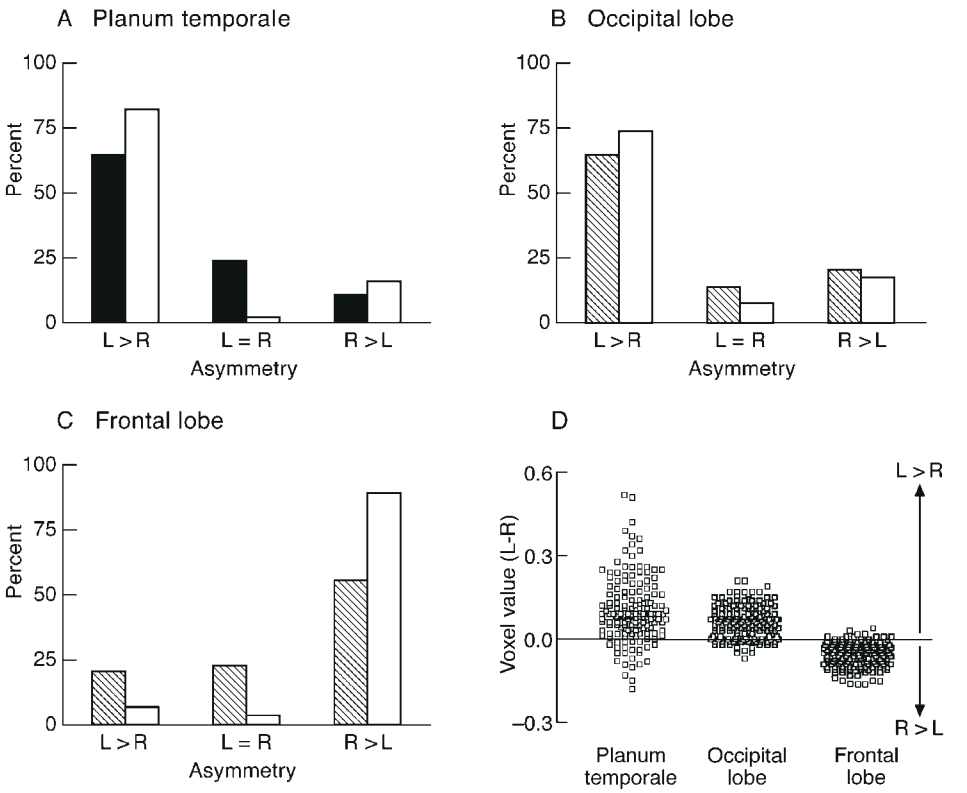

Figure 4. Population distributions for asymmetries in the planum temporale, occipital lobes and frontal lobes. Percent of subjects showing $L > R$, $L = R$ and $R > L$ differences in (*a*) the planum temporale, (*b*) the occipital lobe and (*c*) the frontal lobe; (*d*) total distributions of data for each region. White bars – data from the current study; black bars – data from Geschwind and Levitsky (1968); striped bars – data from LeMay (1984); small squares – data for individual subjects. Voxel values represent between-hemisphere (i.e. within-subject, *L* minus *R*) differences in the smoothed gray matter images. Positive differences indicate more gray matter in the left hemisphere than the right.

amounts of gray matter. The ideal requirement for such a subtraction would be perfect spatial homology between structures in each hemisphere. It is known, however, that the same structure may have a slightly different spatial location in each hemisphere, which may or may not be related to a difference in size. The use of a symmetrical template, linear transformation to this template and smoothing of the data all served to reduce the effect of between hemisphere differences in spatial homology. It is likely also that such within-subject differences are smaller than between-subject differences in the spatial location of structures so the use of a large sample results in spatial averaging of these differences. As already noted, the precautions taken in the image processing stages minimize the likelihood of finding false positive asymmetries but the stringent statistical criteria adopted to control for the number of comparisons increases the likelihood of false negatives.

As described in the Introduction, the asymmetries between the left and right occipital and frontal lobes and between the left and right planum temporale were initially revealed by analysis of post-mortem specimens, measurements of skulls, and analysis of brain scans acquired using computed tomography or MRI (Geschwind and Levitsky, 1968; LeMay, 1977, 1984; Chui and Damasio, 1980; Falk *et al.*, 1991; Steinmetz and Galaburda, 1991). The distributions of these asymmetries in our analysis are comparable with those of previous reports, although they differed in their estimation of the number of subjects who showed symmetry; very few of our subjects had no difference between their left and right hemispheres at these voxels. The method used in our study differs from the previous methods because it does not require *a priori* definition of boundaries and does not involve decisions to be made by a rater. The replication of these established hemispheric asymmetries with similar population distributions demonstrates the validity of this method.

In addition to replicating the presence of the above asymmetries, our analysis revealed several other significant gray matter asymmetries. These are less established in the literature, but in several cases, are consistent with previous observations made in region-of-interest volumetric analyses. For example, the $R > L$ asymmetry of the caudate nucleus reported here, is consistent with region-of-interest studies of this nucleus (Ifthikharuddin *et al.*, 2000). On the medial surface of the frontal lobe, the anterior cingulate sulcus demonstrated $R > L$ asymmetry, and the superior–rostral sulcus $L > R$ asymmetry. These findings are consistent with a previous volumetric analysis of MRI scans (Paus *et al.*, 1996). In the temporal lobe, the uncus, superior temporal sulcus, and inferior temporal gyrus demonstrated $R > L$ asymmetry. A post-mortem study of temporal lobe gyri (Highley *et al.*, 1999) revealed $R > L$ asymmetry for the volume of the middle temporal gyrus; this is consistent with our finding of $R > L$ asymmetry in the superior temporal sulcus.

The inferior portion of the anterior insular cortex demonstrated a highly significant (see Table 2; $t = 10.20$) $R > L$ asymmetry. To our knowledge, there have been no previous reports of such an asymmetry in the insular cortex and, thus, this finding may be novel. There was also a less significant asymmetry (see Table 1; $t = 5.29$) favoring the left hemisphere in a more superior part of the anterior insula. It is likely, therefore, that in a region-of-interest analysis these two asymmetries may

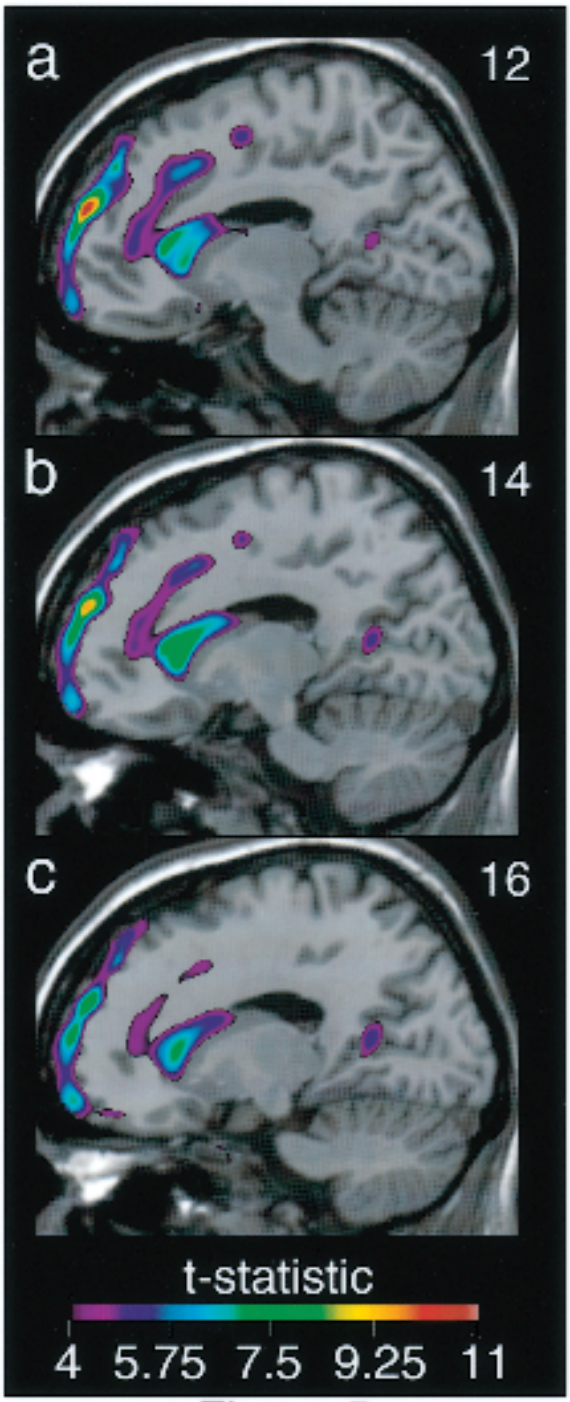

Figure 5

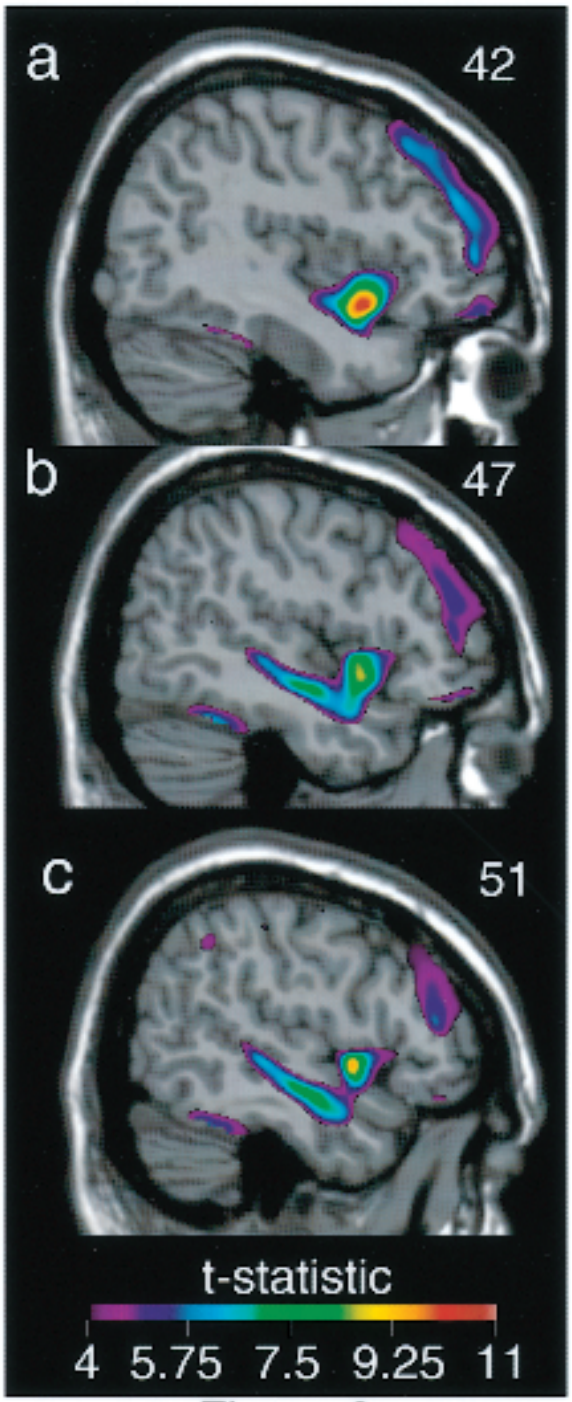

Figure 6

Figure 5. Asymmetry of the anterior cingulate sulcus and caudate nucleus. The map of the *t*-statistic was thresholded at >4.0 and superimposed on sagittal slices through the MRI brain volume of a single subject. The slices shown are from the medial right hemisphere; values of *x* are given in the upper right corner of each image, indicating the distance (in mm) of the image from the parasagittal plane through the midline. Note the shapes and positions of the statistical peaks indicating $R > L$ asymmetry of the cingulate sulcus and the caudate nucleus. Note also the peak in the parietal–occipital fissure.

Figure 6. Asymmetry of the frontal opercular region and superior temporal sulcus. The map of the *t*-statistic was thresholded at >4.0 and superimposed on sagittal slices through the MRI brain volume of a single subject. The slices shown are from the lateral right hemisphere; values of *x* are given in the upper right corner of each image, indicating the distance (in mm) of the image from the parasagittal plane through the midline. Note the presence of $R > L$ asymmetries of the inferior portion of the anterior insula (*a*), the premotor portion of the frontal operculum (*b*), and the superior temporal sulcus (*b* and *c*).

have been combined resulting in an appearance of symmetry for this region. Further analyses are required to confirm and elucidate these asymmetries.

Consistent with the functional specialization of the left hemisphere for language, regions subserving language functions in this hemisphere were shown to have more gray matter than

their counterparts in the right hemisphere. In addition to the planum temporale, such regions included the posterior fusiform and angular gyri. Studies of post-mortem data and MRI analysis in these gyri also report $L > R$ asymmetry in normal healthy individuals (Eidelburg and Galaburda, 1984; McDonald *et al.*, 2000; Niznikiewicz *et al.*, 2000). In view of these $L > R$ asymmetries for posterior language areas, it might be expected that a similar asymmetry existed in the anterior language areas, namely Broca's area or other regions in inferior frontal cortex. Region-of-interest studies of these areas, however, have failed to demonstrate conclusively any structural asymmetry (Tomaiuolo *et al.*, 1999), except for the cortical surface area of the pars triangularis and pars opercularis (Foundas *et al.*, 1998). Our results are consistent with the negative findings for volume differences in this region.

Our analyses failed to reveal any differences in the asymmetry of the two hemispheres according to sex or handedness. This result is somewhat surprising but in accord with the findings of another large sample study of asymmetry of the frontal and occipital lobes (Koff *et al.*, 1986). Other studies, however, have reported sex- and handedness-related differences in hemispheric asymmetries (Bear *et al.*, 1986; Amunts *et al.*, 2000). Our sample was divided fairly evenly according to sex with substantial numbers in each group and should, therefore, have had enough statistical power to reveal differences in asymmetry between the sexes. When the group of male subjects were reanalyzed separately, increases in the *t*-statistics were observed for the asymmetries reported in the initial analysis of all 142 subjects, particularly for the $R > L$ asymmetries in the frontal lobes. This suggests that the degree of asymmetry in these regions is either larger or less variable in males than in females. For handedness, the population demonstrated the normal incidence of left-handedness, namely around 10%. When the 14 left-handed subjects were excluded and the subsample of 128 right-handed subjects was reanalyzed separately, considerable increases in the *t*-statistics were observed for most of the asymmetries reported in the initial analysis. This also suggests that asymmetries in right-handed subjects are either larger or less variable than those in left-handed subjects. Analyses with a larger comparison group of left-handed individuals may reveal significant differences in asymmetries related to cerebral dominance for handedness. The results of these separate analyses emphasize the importance of matching for sex and handedness when comparing asymmetries between groups of subjects.

In order to understand the relationship between functional and structural asymmetries, the basis of the asymmetries demonstrated by this method need to be addressed. Using MRI it is not possible to determine the specific contributions of neurons and glia to the volume of gray matter, but their number, size and density are probable influences. Cytoarchitectural studies have revealed that volume asymmetries in homologous regions are the result of a decrease in neuronal number in the smaller of the two areas (Rosen *et al.*, 1991), probably reflecting unilateral ontogenetic cell loss. Asymmetric areas also have fewer inter-hemispheric connections than symmetric areas, perhaps as a result of increased axonal pruning (Galaburda *et al.*, 1990). Two recent studies of the cytoarchitecture of posterior temporal tissue have revealed asymmetries favoring the left hemisphere in the thickness of the axonal myelin sheath (Anderson *et al.*, 1999) and in the separation between, and amount of non-neuronal space within, cell columns (Buxhoeveden and Casanova, 2000).

Given that several structural asymmetries are present very early in life (Witelson and Pallie, 1973; Chi *et al.*, 1977), it seems likely that they share a genetic basis with functional predispositions and are for the most part independent of the postnatal environment. The known plasticity of the brain, however, suggests that the possibility remains for experience-dependent changes in brain structure (Maguire *et al.*, 2000). Also, not all asymmetries necessarily have a common genetic basis, as suggested by a recent study of patients with *situs inversus totalis* (Kennedy *et al.*, 1999). These patients had the typical left lateralization for language function determined by functional MRI, but reversed frontal and occipital petalia and normal $L > R$ asymmetry of the planum temporale. This led to the suggestion that the genetic basis for the frontal and occipital petalias might be linked to that for other asymmetric visceral organs, whereas the asymmetry of the planum temporale has a different ontogenesis.

We conclude that the method described here is a useful and valid technique for detecting structural asymmetries. The results can be used to direct more detailed searches by traditional region-of-interest methods to determine the precise nature of the asymmetry. This method may also be useful in the study of patient populations in whom abnormal asymmetry is suspected. Statistical analyses such as those presented here are particularly important for patient studies due to the large heterogeneity in such groups. Using a large database such as ours, statistical maps of gray matter differences can be calculated for comparison with individual patients in order to detect regions with anomalous amounts of gray matter (e.g. more than two standard deviations of the mean). Further developmental studies will contribute to our understanding of the relative contributions of pre- and post-natal factors to the ontogenesis of structural asymmetries.

Notes

This study was supported by the International Consortium for Brain Mapping through a grant for Human Brain Project/Neuroinformatics research, which is funded jointly by the National Institute of Mental Health, National Institute of Neurological Disorders and Stroke, National Institute on Drug Abuse, and the National Cancer Institute. We thank Dr Robert Zatorre for useful comments on the manuscript.

Address correspondence to Kate Watkins, Rm 276, Montreal Neurological Institute, 3801 University, Montreal, Quebec H3A 2B4, Canada. Email: kwatkins@bic.mni.mcgill.ca.

References

Amunts K, Jäncke L, Mohlberg H, Steinmetz H, Zilles K (2000) Interhemispheric asymmetry of the human motor cortex related to handedness and gender. Neuropsychologia 38:304–312.

Anderson B, Southern BD, Powers RE (1999) Anatomic asymmetries of the posterior superior temporal lobes: a postmortem study. Neuropsychiatry Neuropsychol Behav Neurol 12:247–254.

Ashburner J, Friston KJ (2000) Voxel-based morphometry — the methods. NeuroImage 11:805–821.

Ashburner J, Hutton C, Frackowiak R, Johnsrude I, Price C, Friston K (1998) Identifying global anatomical differences: deformation-based morphometry. Hum Brain Mapp 6:348–357.

Bear D, Schiff D, Saver J, Greenberg M, Freeman R (1986) Quantitative analysis of cerebral asymmetries. Fronto-occipital correlation, sexual dimorphism and association with handedness. Arch Neurol 43: 598–603.

Broca P (1861) Perte de la parole. Ramollisement chronique et destruction partielle du lobe antérieur gauche du cerveau. Bull Soc Anthrop 2:235–238.

Buxhoeveden D, Casanova M (2000) Comparative lateralisation patterns in the language area of human, chimpanzee, and rhesus monkey brains. Laterality 5:315–330.

Chi JG, Dooling EC, Gilles FH (1977) Gyral development of the human brain. Ann Neurol 1:86–93.

Chui HD, Damasio AR (1980) Human cerebral asymmetries evaluated by computerized tomography. J Neurol Neurosurg Psychiatry 43: 873–878.

Collins DL, Neelin P, Peters TM, Evans AC (1994) Automatic 3D intersubject registration of MR volumetric data in standardized Talairach space. J Comput Assist Tomogr 18:192–205.

Crow TJ (1990) Temporal lobe asymmetries as the key to the etiology of schizophrenia. Schizophr Bull 16:433–443.

Eidelburg D, Galaburda AM (1984) Inferior parietal lobule. Divergent architectonic asymmetries in the human brain. Arch Neurol 41: 843–852.

Falk D, Hildebolt C, Cheverud J, Kohn LA, Figiel G, Vannier M (1991) Human cortical asymmetries determined with 3D MR technology. J Neurosci Methods 39:185–191.

Filipek PA (1995) Neurobiological correlates of developmental dyslexia: how do dyslexics' brains differ from those of normal readers? J Child Neurol 10:S62–S69.

Foundas AL, Eure KF, Luevano LF, Weinberger DR (1998) MRI asymmetries of Broca's area: the pars triangularis and pars opercularis. Brain Lang 64:282–296.

Galaburda AM, Rosen GD, Sherman GF (1990) Individual variability in cortical organization: its relationship to brain laterality and implications to function. Neuropsychologia 28:529–546.

Geschwind N, Levitsky W (1968) Human brain — left–right asymmetries in temporal speech region. Science 161:186–187.

Hendren RL, De Backer I, Pandina GJ (2000) Review of neuroimaging studies of child and adolescent psychiatric disorders from the past 10 years. J Am Acad Child Adolesc Psychiatry 39:815–828.

Highley JR, McDonald B, Walker MA, Esiri MM, Crow TJ (1999) Schizophrenia and temporal lobe asymmetry. Br J Psychiatry 175:127–134.

Ifthikharuddin SF, Shrier DA, Numaguchi Y, Tang X, Ning R, Shibata DK, Kurlan R (2000) MR volumetric analysis of the human basal ganglia: normative data. Acad Radiol 7:627–634.

Kennedy DN, O'Craven KM, Ticho BS, Goldstein AM, Makris N, Henson JW (1999) Structural and functional brain asymmetries in human situs inversus totalis. Neurology 53:1260–1265.

Koff E, Naeser MA, Pieniadz JM, Foundas AL, Levine HL (1986) Computed tomographic scan hemispheric asymmetries in right- and left-handed male and female subjects. Arch Neurol 43:487–491.

LeMay M (1977) Asymmetries of the skull and handedness. Phrenology revisited. J Neurol Sci 32:243–253.

LeMay M (1984) Radiological, developmental and fossil asymmetries. In: Cerebral dominance: the biological foundations (Geschwind N, Galaburda AM, eds), pp. 26–42. Cambridge, MA: Harvard University Press.

Maguire EA, Gadian DG, Johnsrude IS, Good CD, Ashburner J, Frackowiak RS, Frith CD (2000) Navigation-related structural change in the hippocampi of taxi drivers. Proc Natl Acad Sci USA 97:4398–4403.

McDonald B, Highley JR, Walker MA, Herron BM, Cooper SJ, Esiri MM, Crow TJ (2000) Anomalous asymmetry of fusiform and parahippocampal gyrus gray matter in schizophrenia: a postmortem study. Am J Psychiatry 157:40–47.

Niznikiewicz M, Donnino R, McCarley RW, Nestor PG, Iosifescu DV, O'Donnell B, Levitt J, Shenton ME (2000) Abnormal angular gyrus asymmetry in schizophrenia. Am J Psychiatry 157:428–437.

Paus T, Otaky N, Caramanos Z, MacDonald D, Zijdenbos A, D'Avirro D, Gutmans D, Holmes C, Tomaiuolo F, Evans AC (1996) *In vivo* morphometry of the intrasulcal gray matter in the human cingulate, paracingulate, and superior–rostral sulci: hemispheric asymmetries, gender differences and probability maps. J Comp Neurol 376: 664–673.

Paus T, Zijdenbos A, Worsley K, Collins DL, Blumenthal J, Giedd JN, Rapoport JL, Evans AC (1999) Structural maturation of neural pathways in children and adolescents: *in vivo* study. Science 283: 1908–1911.

Petty RG (1999) Structural asymmetries of the human brain and their disturbance in schizophrenia. Schizophr Bull 25:121–139.

Prima S, Thirion JP, Subsol G, Roberts N (1998) Automatic analysis of normal brain dissymmetry in males and females on MRI images. Proceedings of International Conference on Medical Image Computing and Computer-Assisted Intervention (MICCAI), pp. 770–779. Berlin: Springer Verlag.

Rosen GD, Sherman GF, Galaburda AM (1991) Ontogenesis of neocortical asymmetry: a [3H] thymidine study. Neuroscience 41:779–790.

Sharma T, Lancaster E, Sigmundsson T, Lewis S, Takei N, Gurling H, Barta P, Pearlson G, Murray R (1999) Lack of normal pattern of cerebral asymmetry in familial schizophrenic patients and their relatives — The Maudsley Family Study. Schizophr Res 40:111–120.

Sled JG, Zijdenbos AP, Evans AC (1998) A non-parametric method for automatic correction of intensity non-uniformity in MRI data. IEEE Trans Med Imaging 17:87–97.

Steinmetz H, Galaburda AM (1991) Planum temporale asymmetry: in-vivo morphometry affords a new perspective for neuro-behavioral research. Reading Writing 3:331–343.

Talairach J, Tournoux P (1988) Co-planar stereotaxic atlas of the human brain. New York: Thieme Medical.

Tomaiuolo F, MacDonald JD, Caramanos Z, Posner G, Chiavaras M, Evans AC, Petrides M (1999) Morphology, morphometry and probability mapping of the pars opercularis of the inferior frontal gyrus: an *in vivo* MRI analysis. Eur J Neurosci 11:3033–3046.

Vargha-Khadem F, Watkins KE, Price CJ, Ashburner J, Alcock KJ, Connelly A, Frackowiak RS, Friston KJ, Pembrey ME, Mishkin M, Gadian DG, Passingham RE (1998) Neural basis of an inherited speech and language disorder. Proc Natl Acad Sci USA 95:12695–12700.

Westbury CF, Zatorre RJ, Evans AC (1999) Quantifying variability in the planum temporale: a probability map. Cereb Cortex 9:392–405.

Witelson SF, Pallie W (1973) Left hemisphere specialization for language in the newborn. Neuroanatomical evidence of asymmetry. Brain 96:641–646.

Worsley KJ, Marret S, Neelin P, Vandal AC, Friston KJ, Evans AC (1996) A unified statistical approach for determining significant signals in images of cerebral activation. Hum Brain Mapp 4:58–73.

Wright IC, McGuire PK, Poline JB, Travere JM, Murray RM, Frith CD, Frackowiak RS, Friston KJ (1995) A voxel-based method for the statistical analysis of gray and white matter density applied to schizophrenia. NeuroImage 2:244–252.

Zijdenbos AP, Forghani R, Evans AC (1998) Automatic quantification of MS lesions in 3D MRI brain data sets: validation of INSECT. Proceedings of International Conference on Medical Image Computing and Computer-Assisted Intervention (MICCAI), pp. 439–448. Berlin: Springer Verlag.